

Proceedings of the Korean Nuclear Society Spring Meeting
Kori, Korea, May 2000

**Neutron Total Cross-Section Measurements for
Dy and Hf in the Energy Region from 0.002 eV to 100 keV**

G. N. Kim, Y. S. Lee, M. H. Cho, I. S. Ko, W. Namkung
*Pohang Accelerator Laboratory, POSTECH,
San 31, Hygjadong Namgu, Pohang, 790-784, Korea.*

H. J. Cho, K. Kobayashi, S. Yamamoto, Y. Fujita
*Kyoto University,
Kumatori-cho, Sennan-gun, Osaka, 590-0494, Japan*

S. K. Ko
*University of Ulsan,
San 1, Moogedong, Namgu, Ulsan, 680-749, Korea*

Abstract

The neutron total cross-sections of Dy and Hf have been measured in the energy region from 0.002 eV to 100 keV by the neutron time-of-flight method with the 46 MeV electron linear accelerator of the Research Reactor Institute, Kyoto University. A ${}^6\text{Li}$ glass scintillator has been used as a neutron detector and metallic plates of Dy and Hf samples, 0.5 to 5.0 mm thick, have been used for the neutron transmission measurement. The distance from the water-cooled Ta target to the sample changer and to the ${}^6\text{Li}$ glass scintillator is 10.5 m and 22.1 m, respectively. Notch filters consist of Co (132 eV), Ag (5.2 and 16.3 eV) and Mn (336 eV), which have a large resonance peaks in the spectrum, have been used to calibrate the energy and to determine the background levels. The present measurements are in general agreement with the previous ones and the evaluated data in ENDF/B-VI.

1. Introduction

An electron linear accelerator (linac) is a powerful tool to produce intense pulsed neutrons. Most of the electron linear accelerators were constructed for various fundamental research programs including neutron spectroscopy. They have been used for neutron cross-section measurements by the time-of-flight (TOF) method covering the energy range from thermal to a few tens of MeV. Pulsed neutrons

from an electron linear accelerator are suited for measuring energy dependent cross-sections with high resolution using the TOF technique.

Moore [1] and Okamoto [2] measured the total cross-sections of Dy in the thermal energy region by using the transmission method. Sturm et al. [3] obtained the cross-sections from 0.08 eV to 20 eV using the heavy water pile and Bragg reflection method. Brunner et al. [4] obtained the total cross-sections in the energy region from 0.015 eV to 2.5 eV with a fast-chopper installed in a thermal reactor. Knorr et al. [5] reported the total cross-sections in the energy region below 3.2×10^{-3} eV in a reactor. Egelstaff [6] measured the total cross-sections from 144 eV to 36 keV by the TOF method using a fast-chopper.

The total cross-sections of Hf has been measured in the thermal neutron energy region by Joki et al. [7], Berstein et al. [8], Moore [1], and Schermer [9]. Bollinger et al. [10] obtained experimental data from 1 eV to 8 keV. Sherwood et al. [11] and Divadeenam et al. [12] measured the total cross-sections in the energy region from 0.11 keV to 0.15 keV and from 0.12 MeV to 0.64 MeV using a Van-de-Graaff accelerator.

Although these total cross-sections of Dy and Hf have been reported, there exist discrepancies among the data, especially in the resonance energy region. Therefore, there is a need to measure these cross-sections in these relevant energy ranges.

In the present work, the neutron total cross-sections of natural Dy and Hf has been measured by the TOF method based on transmission measurement using the 46 MeV electron linear accelerator of the Research Reactor Institute, Kyoto University (KURRI). A ${}^6\text{Li}$ glass scintillator has been used for neutron detection as in the previous work [13]. The neutron total cross-sections of natural Dy and Hf deduced from the transmission measurement are compared with other measurements and the evaluated data in ENDF/B-VI [14].

2. Experimental Method

2.1. Transmission Samples

In the total cross-section measurements, we used three Dy metal samples and four Hf metal samples. The physical parameters of the transmission samples used in the experiment are given in **Table 1**. The transmission samples were placed at the midpoint of the flight path and were cycled into the neutron beam by an automatic sample changer with four sample-positions. The impurities in the natural Dy sample used in this experiment are less than 0.25%, as shown in **Table 2**.

A set of notch filters of Co, Ag, Mn, and Cd were mounted in front of the sample changer for the energy calibration and the background estimation.

Table 1. Physical parameters of samples used in the experiment.

Sample	Purity (%)	Thickness(mm)		Size (cm ²)
		(atoms/kb)	(mm)	
Dy	99.9	1.584	0.5	5.0 × 5.0
		9.506	3.0	
		15.843	5.0	
Hf	99.9	2.244	0.5	5.0 × 5.0
		6.731	1.5	
		8.975	2.0	
		13.462	3.0	

Table 2. Components of impurities included in sample of natural Dy.

Impurities	Gd	Er	Y	Ho	Tb	Si	Fe	Mg	Ca	Al	Ni	Ta
Contents(%)	<0.01	<0.01	<0.01	<0.01	<0.01	<0.01	<0.01	<0.01	<0.01	0.05	<0.01	<0.1

2.2. Experimental Arrangement

The transmission measurements were made by using the neutron TOF method with the 46 MeV electron linear accelerator at the Research Reactor Institute, Kyoto University (KURRI). The present experimental arrangement is shown in Fig. 1. Bursts of fast neutrons were produced from a water-cooled photoneutron target, which was made of twelve sheets of Ta plates 5 cm in diameter with an effective thickness of about 3 cm. This target was set at the center of an octagonal water tank, which was 30 cm in diameter and 10 cm thick, to moderate the fast neutrons. A shadow bar made of a Pb block, 7 cm thick and 20 cm long, was placed in the neutron flight path in front of the Ta target to reduce the gamma-flash generated by the electron burst in the target. The flight path used in this experiment was in a direction at 90° from the electron beam. The transmission samples were placed at approximately the midpoint of the 22.1 m flight path and were cycled into the neutron beam by using the automatic sample changer with four sample-positions. The neutron collimation system was mainly composed of B₄C-hardened epoxy resin, H₃BO₃ and Pb collimators, which were symmetrically tapered from 10 cm diameter at both the beginning and the end of the flight tube to 4 cm diameter at the middle position where the transmission sample located. For the cross-section measurement in the energy range above 0.5 eV, a 0.5-mm-thick Cd sheet was inserted in the neutron beam to suppress overlap of thermal neutrons from the previous pulses due to the high-frequency operation. During the experiment, the KURRI linac was operated

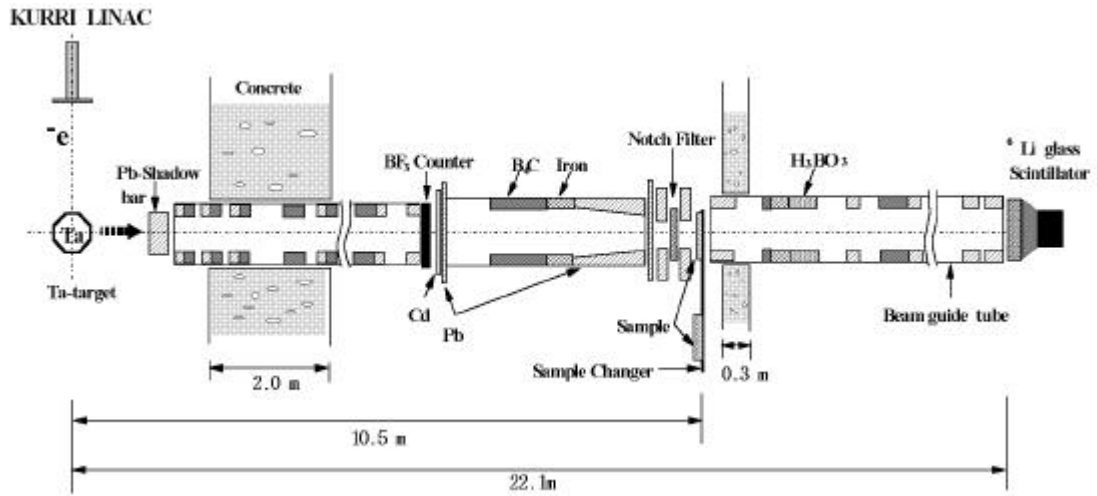


Fig. 1. Experimental setup for the TOF method with the KURRI linac.

in two different modes: One was that without a Cd sheet for the thermal neutron energy region (thermal region) with the linac operating conditions with a repetition rate of 25 Hz, a pulse width of 3 μ s, a peak current of 200 mA, and an electron energy of 30 MeV, and the other was with a Cd sheet for the higher energy region (epicadmium region) with a repetition rate of 100 Hz, a pulse width of 22 ns, a peak current of 1 A, and an electron energy of 30 MeV.

2.3. Neutron Detector

For the TOF spectrum measurement, a ^6Li glass scintillator of 12.7 cm in diameter and 1.27 cm in thickness was mounted on an EMI-9618/R photomultiplier and used as a neutron detector. It was located at a distance of 22.1 ± 0.01 m from the photoneutron target. Neutron signals were amplified, discriminated, and sent to the data acquisition system. The neutron intensity during the TOF measurement was monitored with a BF_3 proportional counter, which was inserted into the neutron beam, as shown in Fig. 1. Neutrons incident on the BF_3 counter produce 478-keV gamma rays (92 % of the time) via the reaction $^{10}\text{B}(n, \alpha)^7\text{Li}$. The resultant pulses are amplified, pass through a window discriminator centered at 478-keV, and are sent to the computer for storage.

3. Data Reduction

3.1 TOF Measurement

For the transmission measurement, three sample-in positions with different thickness samples and a sample-out position (open) were cycled periodically into the neutron TOF beam for preset time intervals by the automatic sample changer.

The cycle time was from 8 to 12 minutes, and the time was allotted to each sample so as to minimize the statistical error in the cross-section measurement.

The TOF signals from the ${}^6\text{Li}$ glass scintillator were fed into a time digitizer, which was initiated by the electron burst of the KURRI linac, and the counts versus TOF channel for each sample position were recorded in each section of the data acquisition system linked to a personal computer. The block diagram of the data acquisition system is shown in Fig. 2. The multi-channel time analyzer was operated as four 2048-channel analyzers corresponding to each transmission sample-in and sample-out positions. Another four 2048-channel analyzers were used for the TOF measurements using the BF_3 monitor system in the TOF beam for normalization of the neutron intensity between the experimental runs.

The channel width of the time analyzer in this experiment was set to $16 \mu\text{s}/\text{ch}$ for the thermal region and $0.5 \mu\text{s}/\text{ch}$ for the epicalcium region. The energy calibration of the TOF neutron beam was performed with the well-known resonance energies at Ag, Co, and Mn filters. Total running times for the thermal and the epi-cadmium regions were about 248 hours.

Each channel I in the time analyzer is converted to the neutron energy E_i as the following relation;

$$E_i = \left\{ \frac{72.3 \times L}{(I - I_0) \times W} \right\}^2 \quad (1)$$

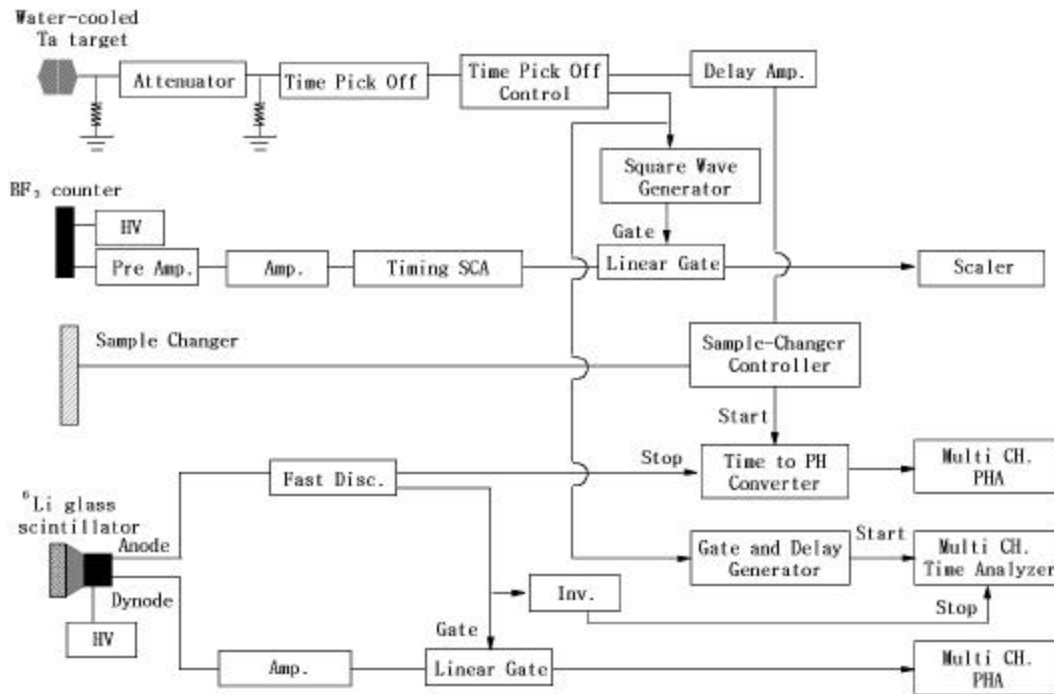


Fig. 2. Block diagram of data acquisition system.

where, L is the neutron flight path in meter, W is the channel width in micro-second, and I_o is the number of channel at the time of flight equals to zero when the neutron burst was produced.

3.2 Background Measurement

In order to estimate the background level, we have used two kinds of method: One was the block-off method using a borated paraffine block of 15 cm in thickness, which was placed in front of the sample to block out the neutron beam. The other was to apply notch-filters of Ag, Co, and Mn and a 0.5 mm -Cd. The magnitude of the background level has been interpolated between the black resonances by using the fitting function $F(I)=aI^b$ where a and b are constants and I is the channel number of the time analyzer. **Fig. 3** shows typical background measurement by the block-off method and the fitting function with notch-filters for the Dy experiment.

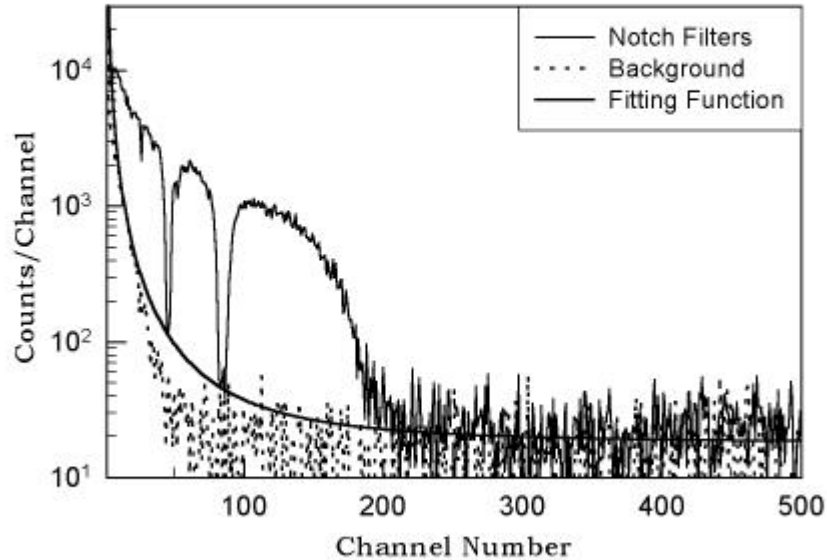


Fig. 3. Background TOF spectrum with a fitting function.

4. Data Analysis

The neutron total cross-section is determined by measuring the transmission of neutrons through the sample. The transmission rate of neutrons of energy E_i is defined as a fraction of incident neutrons passing through the sample as compared to the open beam. Thus, the neutron total cross-section is given as follows, using the neutron transmission rate $T(E_i)$:

$$\sigma(E_i) = \frac{1}{N} \ln T(E_i) \quad (2)$$

$$T(E_i) = \frac{\{I(E_i) - IB(E_i)\}/M}{\{O(E_i) - OB(E_i)\}/MB} \quad (3)$$

where N is the atomic density of the transmission sample, and the bracket (E_i) means the total counts in i -th energy group corresponding to each TOF channel. $I(E_i)$ and $O(E_i)$ are the foreground counts for sample-in and sample-out, $IB(E_i)$ and $OB(E_i)$ are the background counts for sample-in and sample-out, and M and MB are the monitor counts for the foreground and the background runs, respectively. The monitor counts are obtained by integrating TOF counts in each channel corresponding to the relevant energy region.

5. Results and Discussion

The total cross-sections of natural Dy and Hf have been obtained in the energy range from 0.002 eV to 100 keV by the neutron TOF method. The results obtained have been summed up in every U0.01 lethargy width in order to obtain better statistics. In the data processing, the following corrections have been made: The dead time of the time analyzer used in this experiment was estimated to be less than 0.1 sec, and the dead time correction could be neglected in the present work. The effect of attenuation of neutron beam due to the thickness of sample was estimated to be less than 0.01 % for the transmission samples. The total cross-section of the pure sample, σ_T , can be obtained by

$$\sigma_T = \frac{\sigma - M_T \cdot \sum_{i=1}^n (P_i \cdot \sigma_i \cdot M_i^{-1} \times 10^{-6})}{1 - \sum_{i=1}^n (P_i \times 10^{-6})} \quad (4)$$

where σ_T is cross-section of the pure sample, σ is cross-section of the sample with impurities, M_T is atomic weight of sample (g), P_i is contents of impurity i (%), σ_i is the cross-section of the impurity i and M_i is atomic weight of impurity. Using Eq. (4), the effect due to the impurities on the transmission measurement is estimated to be < 0.1 % considering their total cross-section values. The total uncertainty in the present experiment is estimated to be less than 3%. The main sources of the uncertainty are the statistical errors (0.65~1.53 % for Dy, 0.36~1.25 % for Hf), the detection efficiencies (1.85~1.98 %), the geometric factor for the samples (< 0.1 %), and the systematic errors (0.5~1.0 %) including some other corrections.

We have compared total cross-sections of Dy and Hf obtained by two

different background estimation methods mentioned on Sec. 3.2. The ratio of the cross-section values obtained by the fitting function to the block-off method (background level ratio) is almost 1 except the resonance region that is due to the poorer statistics. The present measurements for natural Dy and Hf are compared with other measurements and the evaluated data in the ENDF/B-VI, as seen in Figs. 4 and 5, respectively. The error bars indicate the total uncertainty estimated from the transmission measurements as mentioned above.

For the Dy sample, the present measurement is generally in good agreement with the existing measured and evaluated data as shown in Fig. 4. However, the data measured by Moore [1] and Sailor et al. [16] and the evaluated data in ENDF/B-VI show a tendency to be a little lower than the present result at energies between 0.01 eV and 1.5 eV. In Fig. 4 (a), the data from 0.26 meV to 3.21 meV measured by Knorr et al. [5] are a little higher. The data from 0.015 eV to 2.512 eV by Brunner et al. [4] and from 0.63 meV to 0.02 eV by Okamoto [2] are in good agreement with the present measurement. The data by Moore [1] seem to have a structure around 0.2 eV. The data from 0.1 eV to 1 eV measured by Sturm et al. [3] show a marked discrepancy from the other measurements and the evaluated data in ENDF/B-VI. In Fig. 4 (b) for the total cross-section of Dy, the data from 2.41 eV to 43 eV measured by Carter [17] are in good agreement with the present measurement

For the Hf sample, the present measurement is in good agreement with other data measured by Bernstein et al. [8], Bollinger et al. [10], Okazaki et al. [18], Moore [1], Joki et al. [7], and Schermer [9] and the evaluated data in ENDF/B-VI as shown in Fig. 5. However, our data in the resonance region and above 300 eV region are lower than the evaluated data in ENDF/B-VI. In the resonance energy region, the resonance parameters for Dy and Hf have to be investigated in the future by analyzing the measured data with a computer code in the future.

VI. Conclusions

The neutron total cross-sections of natural Dy and Hf have been measured in the energy region from 0.002 eV to 100 keV by using the neutron TOF method and a ^6Li glass scintillator as a neutron detector. For the Dy, the present measurement is in good agreement with the evaluated data in ENDF/B-VI and other measurements. However, the data from 0.1 eV to 1.0 eV by Sturm *et al.* and from 144 eV to 10 keV by Egelstaff are a little differ from our result. The evaluated data in ENDF/B-VI are higher than the present measurement in the energy range from 500 eV to 2 keV. The evaluated cross-sections of Hf in ENDF/B-VI are higher than the measured cross-section in the energy region above 300 eV, although the evaluation and most of the previous measurements are close

to the present data in general. The data measured in the resonance energy region should be analyzed in the future to get the resonance parameters.

Acknowledgement

The authors would like to express their sincere thanks to the staff of the Research Reactor Institute, Kyoto University (KURRI) for the excellent linac operation. This work was supported partly by the research funds from the Korea Atomic Research Institute and performed under the collaboration between the KURRI and the Pohang Accelerator Laboratory (PAL).

References

- [1] W. M. Moore, Bull. Am. Phys. Soc. **6**, 70 (X11) (1961).
- [2] K. Okamoto, Report JAERI-1069 (1964).
- [3] W. J. Sturm and G. P. Arnold, Phys. Rev. **71**, 556 (1947).
- [4] J. Brunner and F. Widder, Report EIR-123 (1967).
- [5] K. Knorr and W. Schmatz, Atomkernenergie (AKE) **16**(9), 49 (1970).
- [6] P. A. Egelstaff, Proc. Phys. Soc. A **70**, 51 (1957).
- [7] E. G. Joki, J. E. Evans and R. R. Smith, Nucl. Sci. and Engi. **11**, 298 (1961).
- [8] S. Bernstein, L. B. Borst, C. P. Stanford, T. E. Stephenson and J. B. Dial, Phys. Rev. **87**, 487 (1952).
- [9] R. Schermer, AEC reports to the NCSAG, WASH-1031, 16 (1961).
- [10] L. M. bollinger, S. P. Harris, C. T. Hibdon and C. O. Muehlhause, Phys. Rev. **92**, 1527 (1953).
- [11] G. L. Sherwood, A. B. Smith and J. F. Whalen, Nucl. Sci. and Engi. **39**, 67 (1970).
- [12] M. Divadeenam, E. G. Bilpuch and H. W. Newson, Report NCSAC-31, 218 (1970).
- [13] K. Kobayashi, Y. Fujita and I. Kimura, Ann. Nucl. Energy, **15**, 381 (1988).
- [14] (Ed.) R. F. Ross, "Endf-201, ENDF/B-VI Summary Documentation," BNL-NCS-17541, 4th Ed. (ENDF/B-VI) Brookhaven National Laboratory (1991), and "ENDF/B-VI MOD 2 Evaluation," by P. G. Young (1996).
- [15] C. Nordborg and M. Salvatores, "Status of the JEF Evaluated Data Library", Nuclear Data for Science and Technolog, edited by J. K. Dickness (American Nuclear Society, LaGrange, IL, 1994).
- [16] V. L. Sailor, H. H. Landon, and H. L. JR. Foote, Phys. Rev. **96**. 1014 (1954).
- [17] R. S. Carter, Exfor Data File 6424001 (1955).
- [18] A. Okazaki, S. E. Darden and R. B. Walton, Phys. Rev., **93**, 461 (1954).

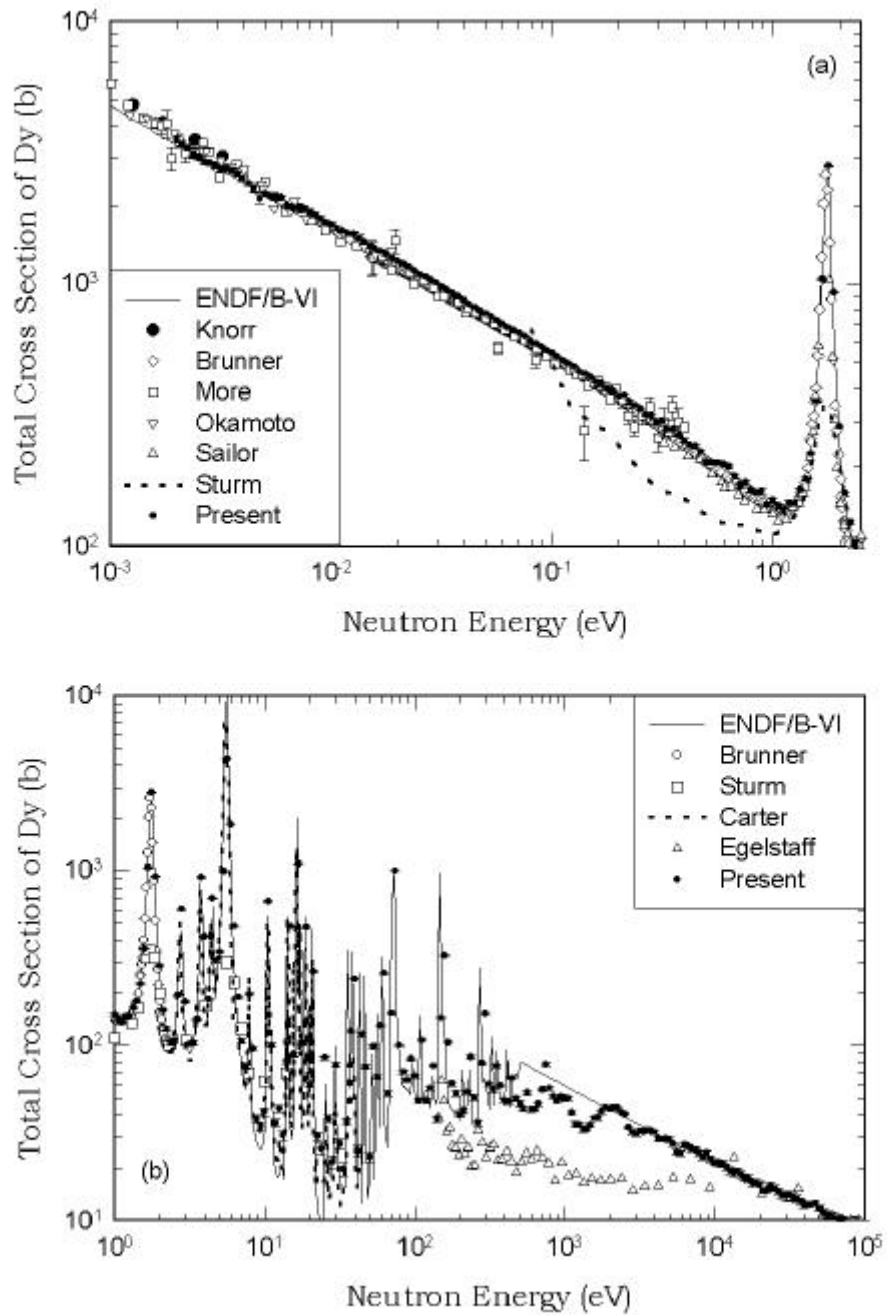


Fig. 4. Comparison of the total cross-section of Dy with the experimental data and the evaluated data: (a) in the lower energy region below 3 eV and (b) in the higher energy region between 1 eV and 0.1 MeV.

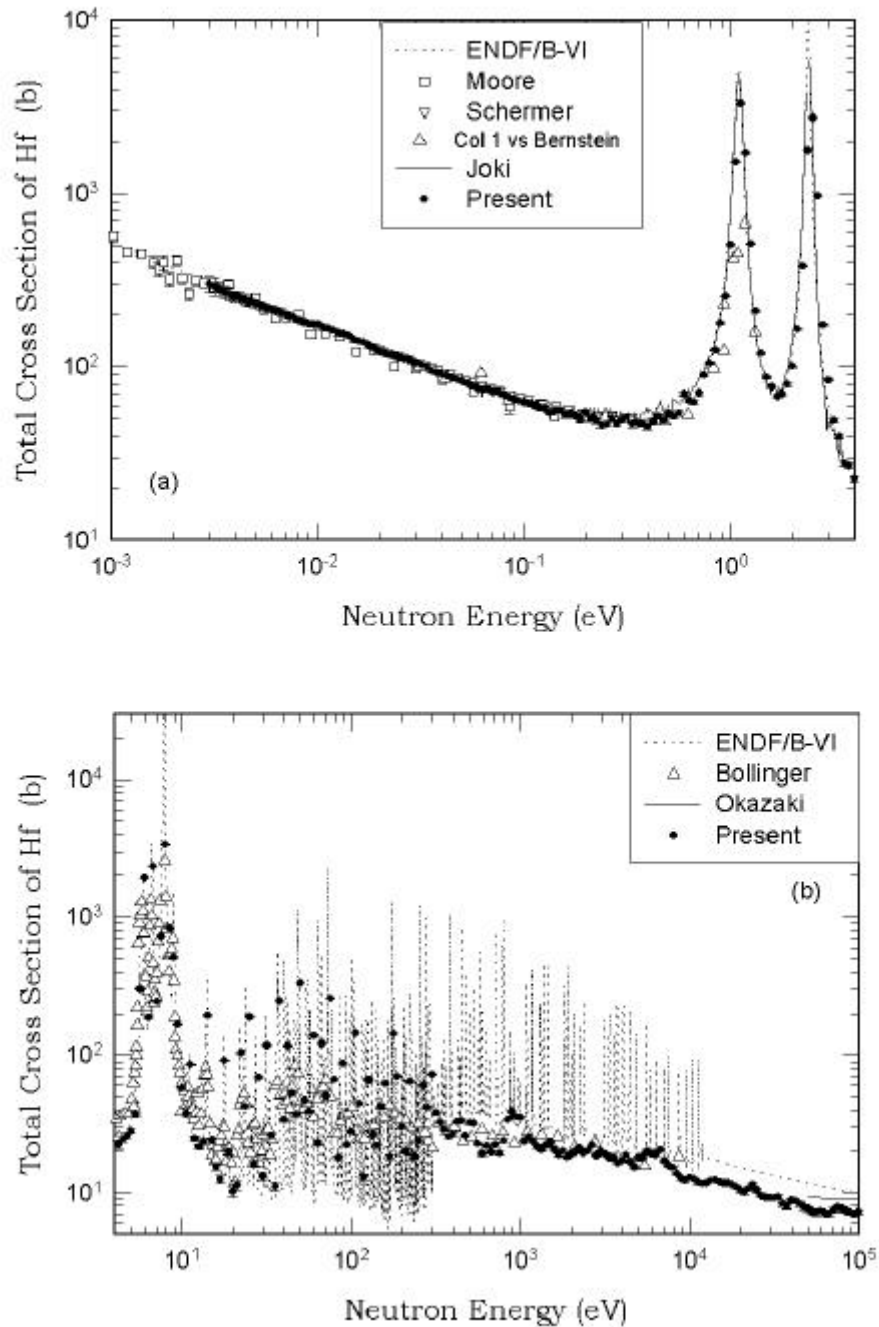


Fig. 5. Comparison of the total cross-section of Hf with the experimental data and the evaluated data: (a) in the lower energy region below 4 eV and (b) in the higher energy region between 4 eV and 0.1 MeV.